Journal of Nuclear Medicine, published on January 6, 2022 as doi:10.2967/jnumed.121.263440

Utility of ^{18}F-rhPSMA-7.3 positron emission tomography for imaging of primary prostate cancer and pre-operative efficacy in N-staging of unfavorable intermediate to very high-risk patients validated by histopathology

Thomas Langbein[1], Hui Wang[1,2], Isabel Rauscher[1], Markus Kroenke[1], Karina Knorr[1], Alexander Wurzer[3], Kristina Schwamborn[4], Tobias Maurer[5], Thomas Horn[6], Bernhard Haller[7], Hans-Jürgen Wester[3], Matthias Eiber[1]

[1]Technical University of Munich, School of Medicine, Klinikum rechts der Isar, Department of Nuclear Medicine; [2]Sichuan University, West China Hospital, Department of Nuclear Medicine; [3]Technical University of Munich, Chair of Radiopharmacy; [4]Technical University of Munich, School of Medicine, Klinikum rechts der Isar, Institute of Pathology; [5]Martini-Klinik and Department of Urology, University Hospital Hamburg-Eppendorf; [6]Technical University of Munich, School of Medicine, Klinikum rechts der Isar, Department of Urology; [7]Technical University of Munich, School of Medicine, Institute of Medical Informatics, Statistics and Epidemiology

First/Corresponding Author: Thomas Langbein, MD, Klinikum rechts der Isar, Ismaninger Straße 22, 81675 Munich, GERMANY, Phone +49.89.4140.2972, Fax +49.89.4140. 4950, Email thomas.langbein@tum.de

Running title: ^{18}F-rhPSMA-7.3 PET/CT primary staging

Word count: 5817

ABSTRACT

^{18}F-rhPSMA-7.3, the lead compound of a new class of radiohybrid prostate-specific membrane antigen (rhPSMA) ligands, is currently in phase III trials for prostate cancer (PCa) imaging. Here, we describe our experience in primary PCa staging. **Methods**. We retrospectively identified 279 patients with primary PCa who underwent ^{18}F-rhPSMA-7.3 PET/CT (staging cohort). A subset of patients (83/279) subsequently underwent prostatectomy with lymph node (LN) dissection without prior treatment (efficacy cohort). Distribution of tumor lesions was determined for the staging cohort and stratified by National Comprehensive Cancer Network (NCCN) risk score. Involvement of pelvic LN was assessed retrospectively by 3 blinded independent central readers, and a majority rule was used for analysis. Standard surgical fields were rated on a five-point scale independently for PET and for morphological imaging. Results were compared to histopathological findings on a patient-, right vs. -left, and template-basis. **Results**. For the staging cohort ^{18}F-rhPSMA-7.3 PET was positive in 275/279 (98.6%), 106/279 (38.0%), 46/279 (16.5%), 65/279 (23.3%) and 5/279 (1.8%) patients for local, pelvic nodal, extrapelvic nodal, metastatic bone, and visceral metastatic disease. In the efficacy cohort, LN metastases were present in 24/83 patients (29%), located in 48/420 (11%) resected templates and in 33/166 (19.9%) hemi-pelvic templates in histopathology. Based on majority vote results, the patient-level sensitivity, specificity and accuracy for pelvic nodal metastases were 66.7% (95%CI, 44.7-83.6%), 96.6% (95%CI, 87.3-99.4%) and 88.0% (95%CI, 78.5-93.8%) for ^{18}F-rhPSMA-7.3 PET and 37.5% (95%CI, 19.6-59.2%), 91.5% (95%CI, 80.6-96.8%) and 75.9% (95%CI, 65.0-84.3%) for morphological imaging, respectively. ^{18}F-rhPSMA-7.3 showed higher interobserver agreement than morphological imaging (patient-level Fleiss' κ=0.54; 95%CI, 0.47-0.62 vs. 0.24; 95%CI, 0.17-0.31).

A mean standardized uptake value ratio of 6.6 (95%CI, 5.2-8.1) documented a high image contrast between local tumors and adjacent low urinary tracer retention. **Conclusion**. ^{18}F-rhPSMA-7.3 PET offers superior diagnostic performance to morphological imaging for primary N-staging of newly diagnosed PCa, shows lower inter-reader variation, and offers good distinction between primary tumor and bladder background activity. With increasing NCCN risk group an increasing frequency of extra-prostatic tumor lesions was observed.

Keywords: ^{18}F-rhPSMA-7.3, positron emission tomography, primary prostate cancer, lymph node metastases, histopathology, interobserver agreement

INTRODUCTION

In recent years, prostate-specific membrane antigen (PSMA) positron emission tomography (PET) with tracers such as ^{68}Ga-PSMA-11 has become increasingly used for diagnostic imaging in patients with prostate cancer (PCa) (*1*). The proPSMA trial established ^{68}Ga-PSMA-11 PET to be a superior imaging modality for patients with primary high-risk PCa compared with conventional imaging but lacks histopathological validation of most lesions (*2*). Most recently, a bicentric phase III trial reported the diagnostic accuracy of ^{68}Ga-PSMA-11 for pelvic N-staging (*3*). In addition to multiple mainly retrospective series, these studies were pivotal for the recent integration of PSMA-ligand PET into various guidelines and for the Food & Drug Administration (FDA)-approval of ^{68}Ga-PSMA-11 (*4-6*).

However, ^{68}Ga-PSMA-11 is not without disadvantages. Rapid urinary excretion results in substantial accumulation in the urinary bladder which can hinder detection of pelvic lesions (*7,8*). Conversely, owing to their longer half-life, potential for larger batch production and their lower positron range resulting in higher image spatial resolution, ^{18}F-labeled PSMA ligands offer a number of logistical benefits and potential for better performance in comparison with their ^{68}Ga-labeled counterparts (*9*). ^{18}F-DCFPyL was recently approved by the FDA for biochemical recurrence (BCR), but it also exhibits high tracer retention in the urinary system (*10,11*).

Radiohybrid PSMA (rhPSMA) ligands are a new class of diagnostic and therapeutic PSMA ligands which can be efficiently labelled with ^{18}F and with radiometals (*12*). Promising preliminary imaging data (*13,14*) have been reported for ^{18}F-rhPSMA-7, which comprises four diastereoisomers. One of these, ^{18}F-rhPSMA-7.3, was selected as the lead rhPSMA compound for

clinical development based on preclinical data (*15*). To date, the safety and biodistribution of ^{18}F-rhPSMA-7.3 have been established in healthy volunteers and PCa patients. ^{18}F-rhPSMA-7.3 has been shown to have low average urinary excretion and diagnostic efficacy has been demonstrated in patients with BCR of PCa (*16-18*). ^{18}F-rhPSMA-7.3 is currently under evaluation in two phase III studies, for primary and BCR PCa (NCT04186845 and NCT04186819).

The present retrospective analysis provides the first data on use of ^{18}F-rhPSMA-7.3 PET for primary staging in patients with newly diagnosed PCa. Specifically, we aimed to describe distribution of tumor lesions stratified by National Comprehensive Cancer Network (NCCN) risk groups (*4*) and to evaluate inter-observer variability and diagnostic performance for pre-operative N-staging in unfavorable intermediate to very high-risk patients.

MATERIAL AND METHODS

Study Design and Patient Populations

We retrospectively extracted data from all patients included in our institution´s database who underwent ^{18}F-rhPSMA-7.3 PET/computed tomography (CT) for primary staging of PCa between November 2018 and April 2020 (Staging Cohort; n=279). To analyze the inter-observer variability and diagnostic efficacy of ^{18}F-rhPSMA-7.3 PET for N-staging validated by histopathology, we selected all patients who underwent subsequent radical prostatectomy and extended pelvic lymph node (LN) dissection (Efficacy Cohort; n=83). Table 1 presents patient

characteristics for both groups. Figure 1 details the cohorts and outlines the clinical, imaging and histopathological data that were collected.

The retrospective analysis was approved by the Ethics Committee of the Technical University Munich (permit 99/19) and the requirement to obtain informed consent was waived. The administration of ^{18}F-rhPSMA-7.3 complied with The German Medicinal Products Act, AMG §13 2b, and the responsible regulatory body (Government of Oberbayern).

^{18}F-rhPSMA-7.3 Synthesis, Administration, and Image Acquisition

^{18}F-rhPSMA-7.3 was synthesized as recently reported *(12)* and administered as an intravenous bolus (median 335, 301-372 MBq) a median 72 (65-80) minutes prior to the scan. Patients underwent ^{18}F-rhPSMA-7.3 PET/CT on a Biograph mCT Flow scanner (Siemens Medical Solutions, Erlangen, Germany) as recently described (*13,14*). All patients received a diagnostic CT scan after i.v. contrast injection (Iomeron 300, weight-adapted, 1.5 mL/kg) and oral intake of diluted contrast medium (300 mg ioxitalamate [Telebrix; Guerbet]). Furosemide (20 mg i.v.) was administered to all patients at the time of ^{18}F-rhPSMA-7.3 injection and patients were asked to void urine prior to the scan. PET scans were acquired in 3D mode with an acquisition time of 2 min per bed position in flow technique (equals 1.1 mm/s). Emission data were corrected for randoms, dead time, scatter, and attenuation and were reconstructed iteratively by an ordered-subsets expectation maximization algorithm (four iterations, eight subsets) followed by a post-reconstruction smoothing Gaussian filter (5 mm full width at one-half maximum).

Image Analysis

In the staging cohort the distribution of tumor lesions was described using the miTNM system from the Prostate Cancer Molecular Imaging Standardized Evaluation (PROMISE) system (*19*). The results for this cohort were taken from the clinical reads. To determine the efficacy for pelvic N-staging, dedicated re-reads of the ^{18}F-rhPSMA-7.3 PET/CT datasets from the efficacy cohort were performed by three board certified nuclear medicine physicians (3-, 6- and 9-years' experience in PSMA-ligand PET). Readers were blinded to the histopathology results. In a first step, the anatomical data using the diagnostic contrast enhanced CT dataset were analyzed by the readers. Next, after an interval of at least 4 weeks, a second read of the corresponding ^{18}F-rhPSMA-7.3 scan was carried out using anatomical images only for anatomical correlation of an area of suspicious uptake to the corresponding LN template. Findings for both reads were reported on a template-level using a five-point Likert scale (1: tumor manifestation; 2: probably tumor manifestation, 3: equivocal, 4: probably benign, 5: benign).

To determine the contrast between local primary tumor uptake and bladder retention of ^{18}F-rhPSMA-7.3, mean standardized uptake values (SUV_{mean}) for ^{18}F-rhPSMA-7.3 were determined within standardized iso-contour volumes of interest with 40% of the SUV_{max}, drawn over the bladder and the primary tumor lesion.

Histopathology

Extended pelvic lymphadenectomy was performed as previously described (*20,21*) to collect right/left common iliac vessel, right/left internal iliac vessel, right/left external iliac vessel and right/left obturator fossa standard LN templates. Further templates (e.g.

presacral/pararectal) were resected if the ^{18}F-rhPSMA-7.3 PET had shown positive LN outside these regions. Uropathologists were blinded to the imaging data.

Statistical Analysis

For quantitative measurements, mean values and standard deviations are presented. ^{18}F-rhPSMA-7.3 PET and morphological imaging results were compared with histopathological results from resected LN on a patient-, right vs. left side, and template-basis. Overall diagnostic accuracy was assessed using receiver operating characteristics (ROC) analyses. Areas under the ROC curves with 95%CI were compared for both ^{18}F-rhPSMA-7.3 PET and morphological imaging. For the patient-based analysis, the method by DeLong (*22*) for two correlated ROC curves was used, and that by Obuchowski (*23*) was used for right vs. left and template-based analyses to account for the multiple assessments within a patient.

A dichotomization of the five-point Likert scale ratings was carried out for analysis of the sensitivity, specificity, and accuracy of the ^{18}F-rhPSMA-7.3 PET and morphological imaging. To reflect a real-world approach, equivocal findings were counted as positive. To estimate cumulative diagnostic results from all three readers a majority vote was used. The results from all three readers dichotomized into negative and positive assessments were compared and in case of any disagreement, the final assessment was based on the majority decision (e.g. 2:1 decision).

For the patient-level analyses, exact confidence intervals were estimated for these measures. For the right vs. left side and template-based analyses, logistic generalized estimating equation models were fitted to the data to account for the correlation of multiple observations within the same patient (*24,25*). For the generalized estimating equation model, an independent

correlation structure was assumed. To investigate a correlation between NCCN risk groups and frequency of extra-prostatic lesions a chi-square test was used. A significance level of 5% was used throughout. All statistical analyses were performed using the statistical software R (*26*), with pROC (*27*) and geepack (*28*).

Inter-observer agreement was evaluated using Fleiss' multi-rater κ (*29*) on a patient-, right vs. left- and template-basis. Ninety-five percent confidence intervals (95%CI) are reported for κ. Interpretation of κ was based on a reproducibility classification provided by Landis and Koch (*30*). Significance between methods is present when the 95%CI are not overlapping.

RESULTS

Distribution of Tumor Lesions on ^{18}F-rhPSMA-7.3 PET

For the staging cohort based on clinical read, ^{18}F-rhPSMA-7.3 PET was positive for local disease in 275/279 (98.6%), for pelvic LN metastases in 106/279 (38.0%), for extrapelvic LN metastases in 46/279 (16.5%), for bone metastases in 65/279 (23.3%) and for visceral metastases in 5/279 (1.8%) patients. On a patient-level, 156 patients had only disease limited to the prostate (N0M0), 42 patients had locoregional LN but no distant metastases (N1M0). In 15 patients, extrapelvic LN but no other distant metastases were present (NxM1a) and 15 patients presented with local tumor and only bone metastases (N0M1b). The distribution of extra-pelvic lesions stratified by NCCN risk group is presented in Figure 2. The patient-based pattern of lesion distribution is presented in Supplementary Table 1. A moderate, but highly significant correlation between risk groups and the frequency of extra-prostatic lesions was found with an increasing

prevalence in higher risk groups (Pearson's chi-squared test for miN1: $\chi^2(5) = 65.6$, $p<0.001$, $\phi = 0.485$; for miM1: $\chi^2(5) = 31.4$, $p<0.001$, $\phi = 0.335$).

Based on clinical read in the efficacy cohort, ^{18}F-rhPSMA-7.3 PET was positive in 82/83 (98.8%) and 20/83 (24.1%) subjects for local and pelvic nodal disease (N1M0). 1 and 6 patients underwent primary surgery with distant metastases being either only extrapelvic nodal (M1a) or only metastatic bone disease (M1b), respectively. Postoperative histopathology showed LN metastases in 24/83 patients, the median size of the largest LN metastasis per patient was 8mm (range 1.5-55).

Diagnostic Accuracy of ^{18}F-rhPSMA-7.3 PET and Morphological Imaging for Pelvic LN **Metastases**

In the efficacy cohort, LN metastases were present in 48/420 (11%) resected templates, in 33/166 (20%) hemi-pelvic templates and in 24/83 patients (29%). A total of 1763 nodes were removed with a median (IQR) of 20 (15-27) per patient. A patient example is presented in Figure 3.

Based on the patient-level majority reads, ^{18}F-rhPSMA-7.3 PET was read positive in 18/83 patients resulting in 16 true positive and 2 false positive cases. It was read negative in 65 patients, including 8 false negative and 57 true negative cases. This resulted in a patient-level sensitivity, specificity and accuracy for pelvic nodal metastases of 66.7% (95%CI, 44.7-83.6%), 96.6% (95%CI, 87.3-99.4%) and 88.0% (95%CI, 78.5-93.8%), respectively. Morphological imaging was read positive in 14/83 patients, resulting in 9 true positive and 5 false positive cases. It was read negative in 69 patients including 15 false negative and 54 true negative cases. The corresponding

patient-level sensitivity, specificity and accuracy were 37.5% (95%CI, 19.6-59.2%), 91.5% (95%CI, 80.6-96.8%) and 75.9% (95%CI, 65.0-84.3%), respectively.

On hemi-pelvic base majority reads, ^{18}F-rhPSMA-7.3 PET was read positive in 25/166 assessments, resulting in 23 true positive and 2 false positive assessments. It was read negative in 141 assessments including 10 false negative and 131 true negative assessments. This resulted in a sensitivity, specificity and accuracy for pelvic nodal metastases on hemi-pelvic base of 69.7% (95%CI, 50.0-84.1%), 98.5% (95%CI, 94.3-99.6%) and 92.8% (95%CI, 87.4-96.0%), respectively. Morphological imaging was read positive in 15/166 assessments resulting in 9 true positive and 6 false positive assessments. It was read negative in 151 assessments including 24 false negative and 127 true negative assessments. The corresponding sensitivity, specificity and accuracy on hemi-pelvis basis were 27.3% (95%CI, 16.5-41.6%), 95.5% (95%CI, 89.3-98.2%) and 81.9% (95%CI, 74.9-87.3%), respectively.

On template-based majority reads, a sensitivity, specificity and accuracy for pelvic nodal metastases of 70.8% (95%CI, 55.6-82.5%), 98.3% (95%CI, 96.6-99.2%) and 95.5% (95%CI, 93.1-97.1%) were found for ^{18}F-rhPSMA-7.3 PET. Morphological imaging showed a template-level sensitivity, specificity and accuracy of 12.5% (95%CI, 6.0-24.3%), 98.3% (95%CI, 96.6-99.2%) and 89.5% (95%CI, 83.9-93.4%), respectively. Detailed results for individual readers are provided in Table 2.

The ROC analysis showed a higher diagnostic performance for ^{18}F-rhPSMA-7.3 compared to morphological imaging for all three readers on both the patient and hemi-pelvic basis. On the patient-level analysis, the differences in the areas under the ROC curves were statistically

significant for reader 1 and 2 on a patient-basis and for all readers on a hemi-pelvic and template basis (Table 3).

Inter-observer Agreement for Pelvic N-staging

Inter-observer agreement was significantly higher for ^{18}F-rhPSMA-7.3 PET compared to morphological imaging for assessment on a patient basis, hemi-pelvic basis and per LN template. The patient-level inter-observer agreement was moderate (Fleiss' κ: 0.54; 95%CI, 0.47-0.62) for ^{18}F-rhPSMA-7.3 PET vs. fair (0.24; 95%CI, 0.17-0.31) for morphological imaging. Similarly, interobserver agreement was moderate for left-sided (0.58; 95%CI, 0.50-0.66) and for right-sided nodes (0.57; 95%CI, 0.49-0.65) in ^{18}F-rhPSMA-7.3 PET, but only fair for left-sided (left: 0.20; 95%CI, 0.12-0.27; right: 0.24; 95%CI, 0.17-0.32) in morphological imaging. Supplementary Figure 1 displays the inter-observer agreements and presents data for template-based assessments.

Uptake in Primary Tumor and Tracer Retention in Urinary Tract

^{18}F-rhPSMA-7.3 uptake in the prostate was present in 82/83 patients who underwent surgery, with a mean SUV_{mean} of 13.0 (range: 2.0-54.4). Retention in the urinary bladder at the time of imaging was rather low with a mean SUV_{mean} of 2.5 (range: 0.9-18.5). Consequently, tumor-to-bladder contrast was high with a mean ratio of 6.6 (range 0.8-40.1) for SUV_{mean}. Data are presented in Table 4 and displayed in Supplementary Figure 2.

DISCUSSION

Here, we present a retrospective analysis on the use of ^{18}F-rhPSMA-7.3 PET/CT for primary staging of newly diagnosed PCa. Distribution of pelvic LN metastases and extrapelvic tumor

lesions in this cohort is clearly associated with NCCN risk groups. In a subset of patients, we determined a high diagnostic performance of ^{18}F-rhPSMA-7.3 PET for N-staging patients with unfavorable intermediate to very high-risk PCa, validated by histopathology. Interobserver agreement of ^{18}F-rhPSMA-7.3 PET for N-staging between three independent readers showed sufficient consistency.

Until today, standard-of-care for N-staging PCa relied on cross-sectional imaging and bone scintigraphy mainly in high-risk PCa (*4*). The reliable detection of LN metastases is especially challenging given the presence of LN metastases in morphologically non-enlarged LN (*31*). Therefore, detection efficacy is low and mainly based on size, with known limitations, especially for LN under 8 mm (*32,33*).

The clinical introduction of PSMA-targeting PET tracers offers a high potential to increase detection of LN metastases and several studies have shown promising results with ^{68}Ga labeled compounds (*34,35*). A prospective, multicenter study compared the accuracy of ^{68}Ga-PSMA-11 PET/CT and conventional imaging with CT and bone scan for primary staging of pelvic LN and distant metastases (*2*). The accuracy of ^{68}Ga-PSMA-11 PET/CT was superior to conventional imaging (92 vs. 65%) and only 15% of patients had a change of clinical management after conventional imaging compared to 28% after ^{68}Ga-PSMA-11 PET/CT. However, the study lacks histopathological validation of LN involvement in a substantial number of patients (only 83/302 patients underwent pelvic LN sampling). Maurer et al. conducted an early retrospective study of ^{68}Ga-PSMA-11 PET for LN staging in 130 patients with intermediate- to high-risk PCa and reported a 65.9% and 68.3% sensitivity, and 98.9% and 99.1% specificity, on patient- and template-based analyses, respectively (*36*).

Similar specificity, but lower sensitivity was reported by Klingenberg et al. in a larger retrospective investigation of newly diagnosed patients with high-risk PCa (37). They reported a sensitivity, specificity, and accuracy of ^{68}Ga-PSMA-11 of 30.6%, 96.5%, and 83.1%, respectively. For ^{68}Ga-PSMA-I&T in 40 patients with intermediate or high-risk disease, Cytawa et al. found a per-region sensitivity, specificity, and accuracy for nodal metastases detection of 35.0%, 98.4%, and 93.0%, respectively (*38*).

Data for the recently approved ^{18}F-DCFPyL from the OSPREY trial that investigated the detection performance for pelvic LN metastases in men with high-risk PCa, showed a specificity ranging from 96-99% across 3 readers, while sensitivity ranged from 31-42% (*11*). Similar to data reported for all other PSMA-ligands, specificity of ^{18}F-rhPSMA-7.3 for pelvic N-metastases is high.

The sensitivity of ^{18}F-rhPSMA-7.3 in this study (e.g., 66.7% on patient-level) appears substantially higher compared to the above mentioned data for ^{68}Ga-PSMA or ^{18}F-DCFPyL. A possible reason might be the nodal lesion size. In the efficacy cohort of our study the median size of the largest LN metastasis per patient was 8 mm. Hope et al. demonstrated a higher sensitivity of ^{68}Ga-PSMA-11 PET in larger pelvic lymph node metastasis >10 mm *(3)*. Comparable findings were shown by the OSPREY trial, where the sensitivity of ^{18}F-DCFPyL was clearly dependent on lesion size. By excluding lesions smaller than 5 mm, sensitivity reached 60.0% (*11*). Potential other factors might also include scanner technique as well as reader experience.

Our retrospective analysis of the novel PSMA-ligand, ^{18}F-rhPSMA-7.3, confirms superiority of PSMA-targeted molecular imaging compared to conventional imaging for N-staging in patients with intermediate to very high-risk primary PCa. ^{18}F-rhPSMA-7.3, achieved an overall accuracy of

88.0%, 92.8% and 95.5% for the patient-level, hemi-pelvic and template analyses, respectively compared with 75.9%, 81.9% and 89.5%, for conventional imaging, respectively.

As expected in clinical routine we observed a clear tendency towards more frequent pelvic and extrapelvic tumor lesions with increasing NCCN group. Comparable findings have been described for the correlation of increasing prostate-specific antigen (PSA) values and the occurrence of bone metastases on bone scintigraphy for PCa staging (*39*), e.g., a prevalence of bone metastases at PSA<10 ng/mL of only 2.3%, 6% at 10>PSA<19.9 ng/mL and 74.9% at PSA>100 ng/mL was found. For PSMA-ligand PET, the mentioned association should be considered crucial, especially in the context of primary N-staging, as nodal involvement in particular can be detected much earlier now, with a high potential to impact clinical management.

^{18}F-rhPSMA-7.3 is a single diastereoisomer of ^{18}F-rhPSMA-7, for which diagnostic accuracy has been well reported. Krönke et al. reported the patient-level sensitivity, specificity and accuracy of ^{18}F-rhPSMA-7 PET to be 72.2%, 92.5% and 86.2%, respectively (*14*), which are comparable with the data in the present study. This supports earlier data which indicate similar diagnostic performance of ^{18}F-rhPSMA-7 and ^{18}F-rhPSMA-7.3 for restaging patients with BCR after radical prostatectomy (*13,18*).

A particular strength of our retrospective analysis was the evaluation of imaging data by 3 independent readers. This allowed us to conduct an inter-observer comparison to determine reproducibility of interpretation of ^{18}F-rhPSMA-7.3 PET compared with morphological imaging. The data show the variability between ^{18}F-rhPSMA-7.3 PET readings is lower than for CT and thus

suggests a more consistent, reader-independent diagnostic performance. Similar high interobserver agreement has been reported for ^{68}Ga-PSMA-11 (*40*).

A well-documented limitation of PSMA-targeting radiotracers such as ^{68}Ga-PSMA-11 and ^{18}F-DCFPyL is a high retention in the urinary system and especially high accumulation in the bladder (*7,8*). For rhPSMA-ligands a low retention in the urinary bladder has been reported (*41*). Our analyses for ^{18}F-rhPSMA-7.3 also revealed low urinary retention and high uptake of tumor lesions resulting in a favorable tumor-to-bladder ratio (mean 6.6). This could potentially increase the detection of local tumor deposits especially in the prostate base.

Our analysis has several limitations. First, it was conducted in a retrospective manner in a limited number of patients. This approach could especially for the efficacy cohort lead to a selection bias given that the cohort of patients who underwent surgery is dependent both on clinical parameters, imaging results and patient´s general health condition and preference. Second, the template-based analysis is limited due to the mapping between a certain LN territory in imaging and the surgical field being prone to errors. Third, histopathological assessment of distant metastases was not available for the majority of patients. ^{18}F-labelled PSMA-ligands like ^{18}F-rhPSMA-7 and ^{18}F-PSMA-1007 have been reported to exhibit a higher number of non-PCa-related uptake than ^{68}Ga-PSMA-11 (*42-45*). However, adequate reader training, interpretation in consensus with cross-sectional imaging, and the clinical context allows differentiation between benign uptake and disease. Fourth, our entire patient cohort does not exclusively contain unfavorable intermediate to high-risk patients. Given local preference and rarely, strong patient request, a few patients in lower NCCN groups underwent ^{18}F-rhPSMA-7.3 for N-staging - typical for a real-world setting.

CONCLUSION

The present study provides real-world clinical evidence to show ^{18}F-rhPSMA-7.3 has moderate-to-high sensitivity and specificity for the detection of LN metastases in patients with intermediate- to very high-risk PCa. The data further show ^{18}F-rhPSMA-7.3 is a more reliable tool than morphological imaging, with lower variability in image interpretation. A distinct association of nodal and extrapelvic tumor involvement with NCCN risk groups was found. ^{18}F-rhPSMA-7.3 compares well with other PSMA-ligands and shows potential for a good differentiation between primary tumor uptake and background bladder retention.

DISCLOSURE

Patent application for rhPSMA (HJW, AW and ME). HJW and ME received funding from Blue Earth Diagnostics Ltd (BED), Oxford, UK (Licensee for rhPSMA) as part of an academic collaboration. HJW is founder, shareholder, and advisor board member of Scintomics GmbH, Fuerstenfeldbruck, Germany. ME reports prior consulting activities for BED, Novartis, Telix, Progenics, Bayer, Point Biopharma and Janssen. No other potential conflicts of interest relevant to this article exist.

ACKNOWLEDGEMENT

Editorial support was provided by Dr C Turnbull (BED).

KEY POINTS

Question: What is the diagnostic efficacy of ^{18}F-rhPSMA-7.3 for N-staging patients with intermediate- to very high-risk prostate cancer in the primary setting?

Pertinent Findings: This retrospective study shows that ^{18}F-rhPSMA-7.3 PET provides superior N-staging of high-risk primary prostate cancer compared with morphological imaging. The efficacy of ^{18}F-rhPSMA-7.3 compares well with published data for other PSMA ligands and offers a good tumor-to-bladder uptake ratio.

Implications for patient care: ^{18}F-rhPSMA-7.3 PET can significantly improve primary N-staging vs conventional imaging.

REFERENCES

1. Lawhn-Heath C, Salavati A, Behr SC, et al. Prostate-specific membrane antigen PET in prostate Cancer. *Radiology.* 2021;299:248-260.

2. Hofman MS, Lawrentschuk N, Francis RJ, et al. Prostate-specific membrane antigen PET-CT in patients with high-risk prostate cancer before curative-intent surgery or radiotherapy (proPSMA): a prospective, randomised, multicentre study. *Lancet.* 2020;395:1208-1216.

3. Hope TA, Eiber M, Armstrong WR, et al. Diagnostic accuracy of ^{68}Ga-PSMA-11 PET for pelvic nodal metastasis detection prior to radical prostatectomy and pelvic lymph node dissection: A multicenter prospective phase 3 imaging trial. *JAMA Oncol.* 2021;7:1635-1642.

4. NCCN. NCCN clinical practice guidelines in oncology: prostate cancer. Version 1.2022. https://www.nccn.org/professionals/physician_gls/pdf/prostate.pdf. 2021. Accessed December 15, 2021.

5. German S3 Guideline. S3-Leitlinie Prostatakarzinom. Version 6.1. https://www.leitlinienprogramm-onkologie.de/fileadmin/user_upload/Downloads/Leitlinien/Prostatatkarzinom/Version_6/LL_Prostatakarzinom_Langversion_6.1.pdf. 2021. Accessed December 15, 2021.

6. FDA. FDA approves first PSMA-targeted PET imaging drug for men with prostate cancer: https://www.fda.gov/news-events/press-announcements/fda-approves-first-psma-targeted-pet-imaging-drug-men-prostate-cancer. 2020. Accessed December 15, 2021.

7. Fendler WP, Eiber M, Beheshti M, et al. ^{68}Ga-PSMA PET/CT: Joint EANM and SNMMI procedure guideline for prostate cancer imaging: version 1.0. *EJNMMI.* 2017;44:1014-1024.

8. Heusser T, Mann P, Rank CM, et al. Investigation of the halo-artifact in ^{68}Ga-PSMA-11-PET/MRI. *PLoS One.* 2017;12:e0183329.

9. Werner RA, Derlin T, Lapa C, et al. ^{18}F-Labeled, PSMA-targeted radiotracers: Leveraging the advantages of radiofluorination for prostate cancer molecular imaging. *Theranostics.* 2020;10:1-16.

10. FDA. FDA approves second PSMA-targeted PET imaging drug for men with prostate cancer: https://www.fda.gov/drugs/drug-safety-and-availability/fda-approves-second-psma-targeted-pet-imaging-drug-men-prostate-cancer. 2021. Accessed December 15, 2021.

11. Pienta KJ, Gorin MA, Rowe SP, et al. A Phase 2/3 prospective multicenter study of the diagnostic accuracy of prostate specific membrane antigen PET/CT with ^{18}F-DCFPyL in prostate cancer patients (OSPREY). *J Urol.* 2021;206:52-61.

12. Wurzer A, DiCarlo D, Schmidt A, et al. Radiohybrid ligands: a novel tracer concept exemplified by ^{18}F- or ^{68}Ga-labeled rhPSMA-inhibitors. *J Nucl Med.* 2019;61:735-742.

13. Eiber M, Kronke M, Wurzer A, et al. ^{18}F-rhPSMA-7 positron emission tomography for the detection of biochemical recurrence of prostate cancer following radical prostatectomy. *J Nuc Med.* 2019;61:696-701.

14. Kronke M, Wurzer A, Schwamborn K, et al. Histologically-confirmed diagnostic efficacy of ^{18}F-rhPSMA-7 positron emission tomography for N-staging of patients with primary high risk prostate cancer. *J Nuc Med.* 2019;61:710-715.

15. Wurzer A, Parzinger M, Konrad M, et al. Preclinical comparison of four [^{18}F, natGa]rhPSMA-7 isomers: influence of the stereoconfiguration on pharmacokinetics. *EJNMMI Research.* 2020;10:149.

16. Tolvanen T, Kalliokoski KK, Malaspina S, et al. Safety, biodistribution and radiation dosimetry of ^{18}F-rhPSMA-7.3 in healthy adult volunteers. *J Nucl Med.* 2021;62:679-684.

17. Malaspina S, Oikonen V, Kuisma A, et al. Kinetic analysis and optimisation of ^{18}F-rhPSMA-7.3 PET imaging of prostate cancer. *EJNMMI.* 2021;48:3723-3731.

18. Rauscher I, Karimzadeh A, Schiller K, et al. Detection efficacy of ^{18}F-rhPSMA-7.3 PET/CT and impact on patient management in patients with biochemical recurrence of prostate cancer after radical prostatectomy and prior to potential salvage treatment. *J Nucl Med.* 2021;62:1719-1726.

19. Eiber M, Herrmann K, Calais J, et al. Prostate cancer molecular imaging standardized evaluation (PROMISE): Proposed miTNM classification for the interpretation of PSMA-ligand PET/CT. *J Nucl Med.* 2018;59:469-478.

20. Heck MM, Retz M, Bandur M, et al. Topography of lymph node metastases in prostate cancer patients undergoing radical prostatectomy and extended lymphadenectomy: results of a combined molecular and histopathologic mapping study. *Eur Urol.* 2014;66:222-229.

21. Maurer T, Souvatzoglou M, Kubler H, et al. Diagnostic efficacy of [^{11}C]choline positron emission tomography/computed tomography compared with conventional computed tomography in lymph node staging of patients with bladder cancer prior to radical cystectomy. *Eur Urol.* 2012;61:1031-1038.

22. DeLong ER, DeLong DM, Clarke-Pearson DL. Comparing the areas under two or more correlated receiver operating characteristic curves: a nonparametric approach. *Biometrics.* 1988;44:837-845.

23. Obuchowski NA. Nonparametric analysis of clustered ROC curve data. *Biometrics.* 1997;53:567-578.

24. Smith PJ, Hadgu A. Sensitivity and specificity for correlated observations. *Stat Med.* 1992;11:1503-1509.

25. Zeger SL, Liang KY. Longitudinal data analysis for discrete and continuous outcomes. *Biometrics.* 1986;42:121-130.

26. The R project. The R project for statistical computing; https://www.R-project.org/. Accessed December 15, 2021.

27. Robin X, Turck N, Hainard A, et al. pROC: an open-source package for R and S+ to analyze and compare ROC curves. *BMC Bioinformatics.* 2011;12:77.

28. Højsgaard S, Halekoh U, Yan J. The R package geepack for generalized estimating equations. *J Statistical Software.* 2005;15:1-11.

29. Hale CA, Fleiss JL. Interval estimation under two study designs for kappa with binary classifications. *Biometrics* 1993;49:523-534.

30. Landis JR, Koch GG. The measurement of observer agreement for categorical data. *Biometrics.* 1977;33:159-174.

31. Heesakkers RA, Hovels AM, Jager GJ, et al. MRI with a lymph-node-specific contrast agent as an alternative to CT scan and lymph-node dissection in patients with prostate cancer: a prospective multicohort study. *Lancet Oncol.* 2008;9:850-856.

32. Hovels AM, Heesakkers RA, Adang EM, et al. The diagnostic accuracy of CT and MRI in the staging of pelvic lymph nodes in patients with prostate cancer: a meta-analysis. *Clin Radiol.* 2008;63:387-395.

33. Mottet N, Bellmunt J, Briers E, et al. The EAU prostate cancer guidelines. http://uroweb.org/guideline/prostate-cancer/. *The EAU.* 2020. Accessed December 15, 2021.

34. von Eyben FE, Picchio M, von Eyben R, Rhee H, Bauman G. ^{68}Ga-Labeled prostate-specific membrane antigen ligand positron emission tomography/computed tomography for prostate cancer: A systematic review and meta-analysis. *Eur Urol Focus.* 2018;4:686-693.

35. Petersen LJ, Zacho HD. PSMA PET for primary lymph node staging of intermediate and high-risk prostate cancer: an expedited systematic review. *Cancer Imaging.* 2020;20:10.

36. Maurer T, Gschwend JE, Rauscher I, et al. Diagnostic efficacy of ^{68}Gallium-PSMA positron emission tomography compared to conventional imaging for lymph node staging of 130 consecutive patients with intermediate to high risk prostate cancer. *J Urol.* 2016;195:1436-1443.

37. Klingenberg S, Jochumsen MR, Ulhoi BP, et al. ^{68}Ga-PSMA PET/CT for primary lymph node and distant metastasis NM staging of high-risk prostate cancer. *J Nucl Med.* 2021;62:214-220.

38. Cytawa W, Seitz AK, Kircher S, et al. ^{68}Ga-PSMA I&T PET/CT for primary staging of prostate cancer. *EJNMMI.* 2020;47:168-177.

39. Abuzallouf S, Dayes I, Lukka H. Baseline staging of newly diagnosed prostate cancer: a summary of the literature. *J Urol.* 2004;171:2122-2127.

40. Fendler WP, Calais J, Allen-Auerbach M, et al. ^{68}Ga-PSMA-11 PET/CT interobserver agreement for prostate cancer assessments: An international multicenter prospective study. *J Nucl Med.* 2017;58:1617-1623.

41. Oh SW, Wurzer A, Teoh EJ, et al. Quantitative and qualitative analyses of biodistribution and PET image quality of a novel radiohybrid PSMA, ^{18}F-rhPSMA-7, in patients with prostate cancer. *J Nucl Med.* 2020;61:702-709.

42. Grünig H, Maurer A, Thali Y, et al. Focal unspecific bone uptake on [^{18}F]-PSMA-1007 PET: a multicenter retrospective evaluation of the distribution, frequency, and quantitative parameters of a potential pitfall in prostate cancer imaging. *EJNMMI.* 2021;48:4483-4494.

43. Arnfield EG, Thomas PA, Roberts MJ, et al. Clinical insignificance of [^{18}F]PSMA-1007 avid non-specific bone lesions: a retrospective evaluation. *EJNMMI.* 2021;48:4495-4507.

44. Kroenke M, Mirzoyan L, Horn T, et al. Matched-pair comparison of ^{68}Ga-PSMA-11 and ^{18}F-rhPSMA-7 PET/CT in patients with primary and biochemical recurrence of prostate cancer: Frequency of non-tumor-related uptake and tumor positivity. *J Nucl Med.* 2021;62:1082-1088.

45. Rauscher I, Krönke M, König M, et al. Matched-pair comparison of ^{68}Ga-PSMA-11 PET/CT and ^{18}F-PSMA-1007 PET/CT: Frequency of pitfalls and detection efficacy in biochemical recurrence after radical prostatectomy. *J Nucl Med.* 2020;61:51-57.

TABLES

Table 1. Patient characteristics of all patients undergoing ^{18}F-rhPSMA-7.3 PET/CT for primary staging (Staging Cohort) and all patients undergoing surgery at our institution without prior neoadjuvant treatment (Efficacy Cohort) between November 2018 and April 2020.

Characteristic	Staging cohort	Efficacy cohort
Patients, N (%)	279 (100%)	83 (29.7%)
Age, y		
Median	70	66
Interquartile range	63-76	62-74
Prostate-specific antigen, ng/mL[*,†]		
Median	13.0	11
Interquartile range	7.2-26.9	7.0-17.8
ISUP Grading[§]		
1	13 (4.7%)	0 (0%)
2	46 (16.5%)	15 (18.1%)
3	61 (21.9%)	25 (30.1%)
4	65 (23.3%)	23 (27.7%)
5	85 (30.5%)	19 (22.9%)
Neoadjuvant treatment before PET/CT, N (%)	16 (5.7%)	0 (0%)
NCCN risk group		
very low	1 (0.4%)	0 (0.0%)
low	7 (2.5%)	0 (0.0%)
favorable intermediate	18 (6.5%)	0 (0.0%)
unfavorable intermediate	74 (26.5%)	36 (43.4%)
high	107 (38.4%)	32 (38.6%)
very high	72 (25.8%)	15 (18.1%)
Time between PET/CT and surgery (days)		
Median		29
IQR		15-46
Pathological T-stage, n (%)		
≤ pT2c		28 (33.7%)
pT3a		18 (21.7%)
≥ pT3b		37 (44.6%)
Pathological N-stage		
pN0		59 (71.1%)
pN1		24 (28.9%)
Median size of largest LN metastasis per patient, mm (range)		8 (1.5-55)

CT, computed tomography; ISUP, International Society of Urological Pathology; NCCN, National Comprehensive Cancer Network; PET, positron emission tomography. [*]At time of imaging; [†]PSA levels were unavailable for 2 patients of the staging cohort; [§]ISUP gradings were unavailable for 9 patients in the staging cohort and for 1 patient in the efficacy cohort.

Table 2. Histologically verified diagnostic accuracy of ^{18}F-rhPSMA-7.3 PET and morphological imaging for pre-operative N-staging

		^{18}F-rhPSMA-7.3 PET/CT			**Morphological imaging**		
	Reader	Sensitivity % (95%CI)	Specificity % (95%CI)	Accuracy % (95%CI)	Sensitivity % (95%CI)	Specificity % (95%CI)	Accuracy % (95%CI)
Patient base	**1**	66.7% (44.7-84.4%)	94.9% (85.9-98.9%)	86.7% (77.5-93.2%)	29.2% (12.6-51.1%)	94.9% (85.9-98.9%)	75.9% (65.3-84.6%)
	2	70.8% (48.9-87.4%)	96.6% (88.3-99.6%)	89.2% (80.4-94.9%)	41.7% (22.1-63.4%)	89.8% (79.2-96.2%)	75.9% (65.3-84.6%)
	3	66.7% (44.7-84.4%)	94.9% (85.9-98.9%)	86.7% (77.5-93.2%)	58.3% (36.6-77.9%)	84.7% (73.0-92.8%)	77.1% (66.6-85.6%)
	Majority vote	**66.7% (44.7-83.6%)**	**96.6% (87.3-99.4%)**	**88.0% (78.5-93.8%)**	**37.5% (19.6-59.2%)**	**91.5% (80.6-96.8%)**	**75.9% (65.0-84.3%)**
Right- vs. left-base	**1**	69.7% (50.0-84.1%)	97.7% (93.3-99.3%)	92.2% (86.7-95.5%)	21.1% (11.1-36.6%)	97.7% (93.3-99.3%)	82.5% (75.3-88.0%)
	2	69.7% (50.0-84.1%)	97.0% (90.5-99.1%)	91.6% (85.1-95.4%)	30.3% (19.4-43.9%)	94.0% (86.8-97.4%)	81.3% (74.3-86.7%)
	3	69.7% (50.0-84.1%)	97.0% (90.6-99.1%)	91.6% (85.6-95.2%)	42.4% (28.4-57.8%)	90.2% (83.5-94.4%)	80.7% (73.8-86.2%)
	Majority vote	**69.7% (50.0-84.1%)**	**98.5% (94.3-99.6%)**	**92.8% (87.4-96.0%)**	**27.3% (16.5-41.6%)**	**95.5% (89.3-98.2%)**	**81.9% (74.9-87.3%)**
Template base	**1**	62.5% (48.5-74.7%)	97.6% (95.5-98.8%)	94.0% (91.0-96.1%)	10.4% (4.5-22.2%)	99.0% (97.5-99.6%)	90.0% (84.2-93.8%)
	2	64.6% (50.3-76.6%)	97.6% (95.2-98.8%)	94.2% (91.2-96.2%)	18.7% (11.9-28.4%)	97.9% (95.5-99.0%)	89.7% (84.7-93.3%)
	3	70.8% (55.6-82.5%)	97.6% (95.0-98.9%)	94.9% (92.1-96.7%)	18.7% (8.8-35.7%)	96.9% (94.9-98.1%)	88.9% (83.2-92.8%)
	Majority vote	**70.8% (55.6-82.5%)**	**98.3% (96.6-99.2%)**	**95.5% (93.1-97.1%)**	**12.5% (6.0-24.3%)**	**98.3% (96.6-99.2%)**	**89.5% (83.9-93.4%)**

CT, computed tomography; PET, positron emission tomography.

Table 3. DeLong's test for correlated ROC

	Reader	^{18}F-rhPSMA-7.3 PET/CT AUC (95%CI)	Morphological imaging AUC (95%CI)	P value
Patient basis	**1**	0.821 (0.716-0.926)	0.724 (0.606-0.843)	0.09774
	2	0.850 (0.738-0.963)	0.672 (0.526-0.817)	0.01226
	3	0.829 (0.720-0.939)	0.779 (0.662-0.896)	0.2785
Right- vs. left-basis	**1**	0.841 (0.745-0.938)	0.699 (0.597-0.800)	0.01195
	2	0.853 (0.762-0.944)	0.657 (0.557-0.757)	0.00041
	3	0.817 (0.708-0.925)	0.699 (0.602-0.795)	0.02655
Template basis	**1**	0.796 (0.726-0.865)	0.645 (0.579-0.712)	$6.879e^{-05}$
	2	0.822 (0.759-0.885)	0.652 (0.568-0.736)	0.00045
	3	0.847 (0.772-0.922)	0.630 (0.551-0.710)	$1.062e^{-07}$

AUC, area under receiver operating curve; CT, computed tomography; PET, positron emission tomography.

Table 4. ^{18}F-rhPSMA-7.3 SUV_{max} and SUV_{mean} for the primary tumors and urinary bladder

	Primary tumor (n=82)		Urinary bladder (n=82)		Ratio primary tumor/urinary bladder (n=82)	
	SUV_{max}	SUV_{mean}	SUV_{max}	SUV_{mean}	Ratio SUV_{max}	Ratio SUV_{mean}
Mean	22.4	13.0	4.3	2.5	6.6	6.6
95%CI	18.3-26.4	10.5-15.65	3.5-5.1	2.0-3.0	5.2-8.0	5.2-8.1
Range	3.6-86.9	2.0-54.4	1.6-31.4	0.9-18.5	0.8-34.2	0.8-40.1

SUV, standardized uptake value

FIGURES

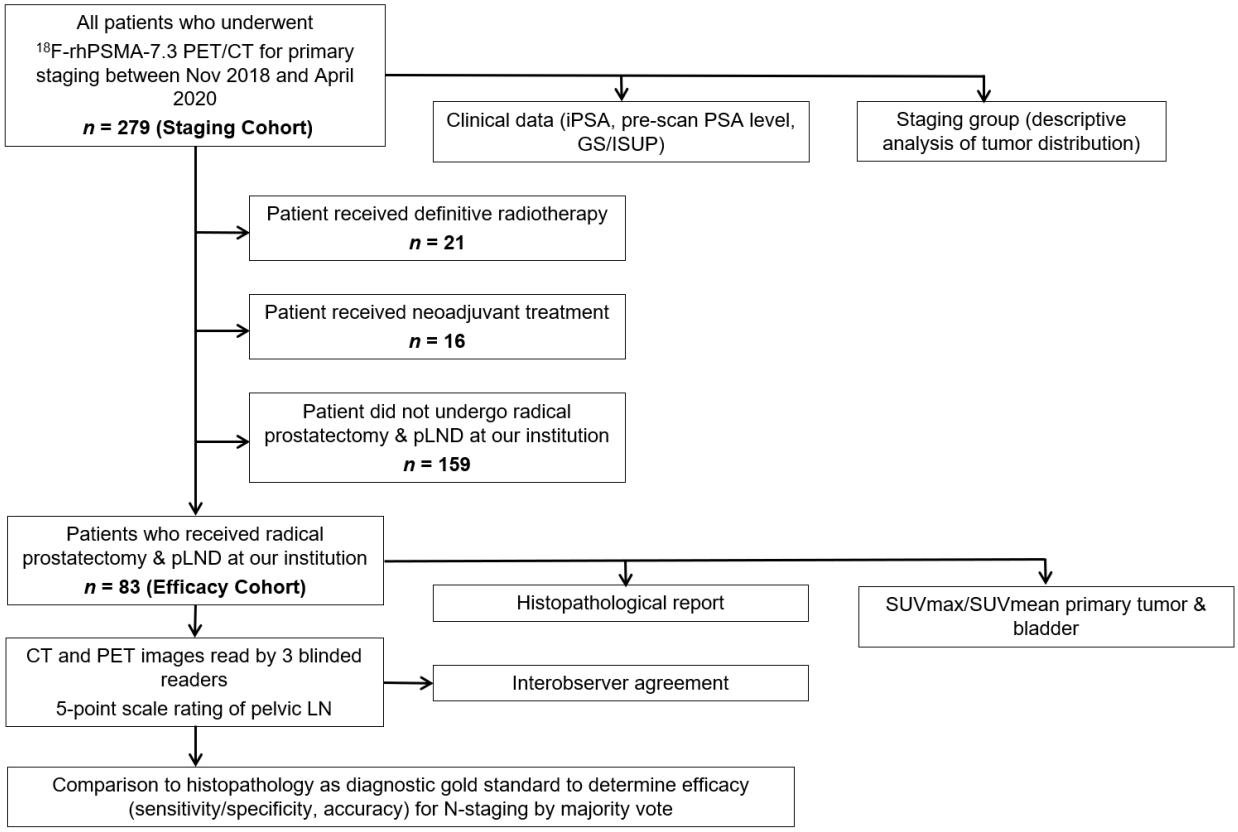

CT, computed tomography; GS, Gleason score; iPSA, initial prostate-specific antigen; ISUP, International Society of Urological Pathology; PET, positron emission tomography; pLND, pelvic lymph node dissection PSA, prostate-specific antigen; SUV, standardized uptake value.

Figure 1. Flow chart of patient selection and data analysis

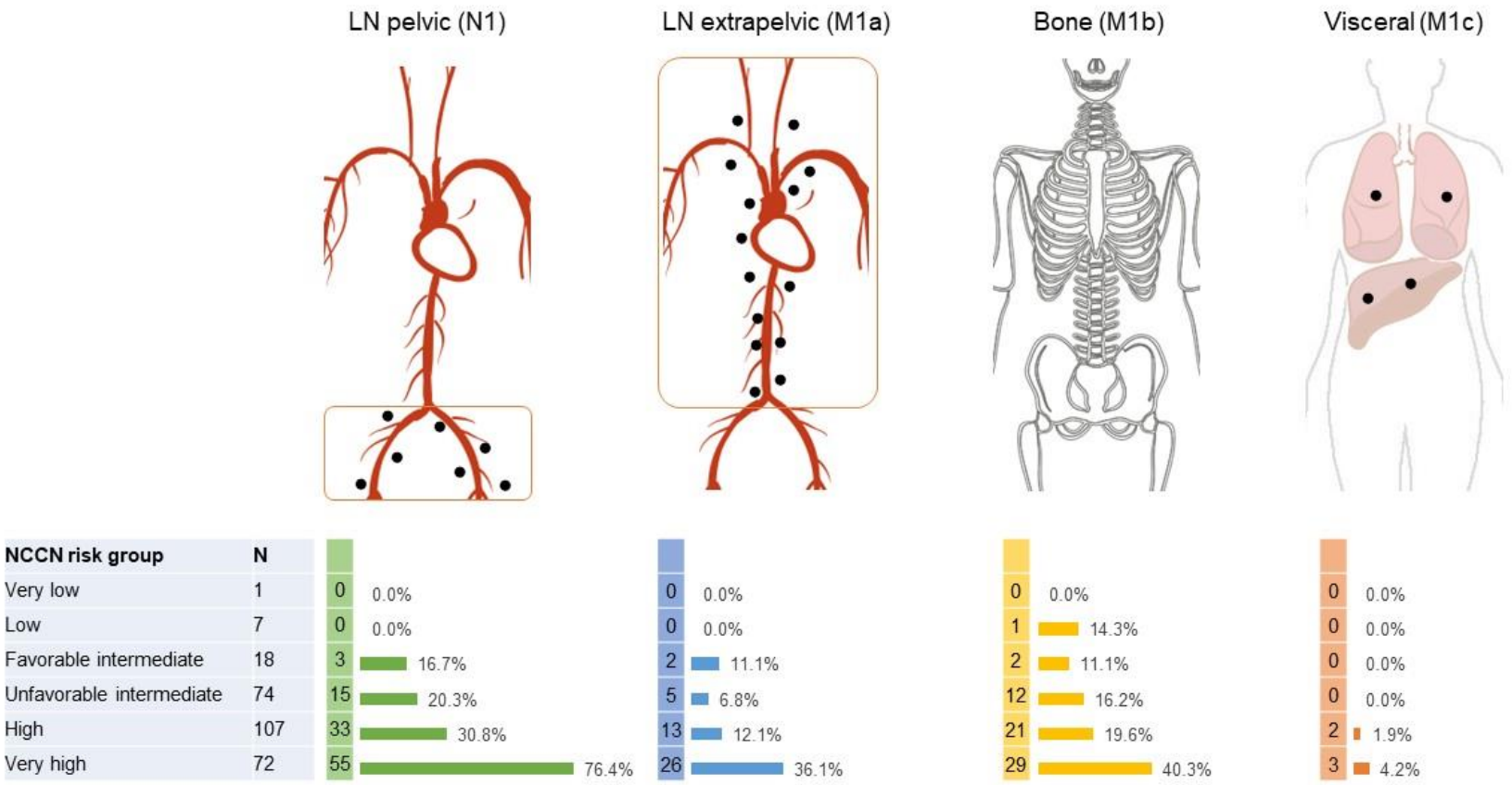

Figure 2. Distribution of extraprostatic tumor lesions in the staging cohort (n=279)

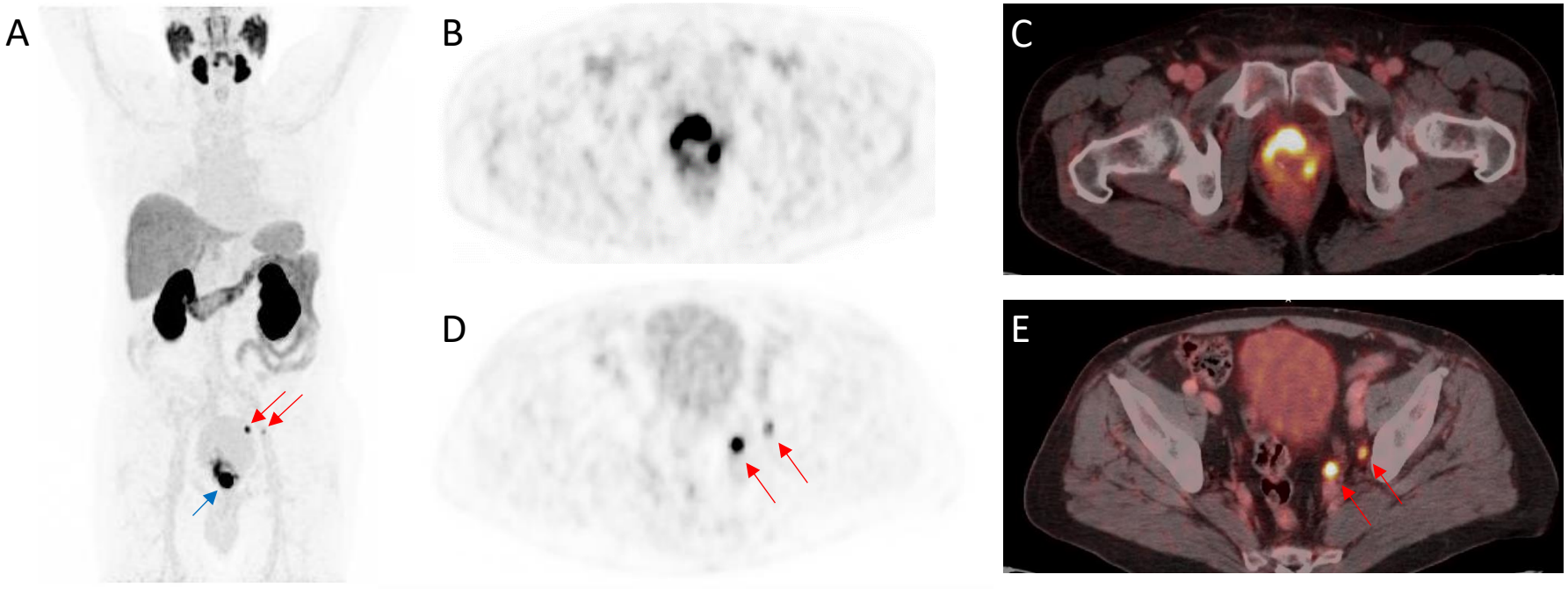

Figure 3. 72-year-old patient with high-risk prostate cancer (iPSA 44 ng/mL) who underwent ^{18}F-rhPSMA-7.3 PET/CT illustrating the primary tumor (blue arrow) and pelvic LN metastases (red arrows) histologically confirmed by radical prostatectomy (pT3b pN1 (2/34), Gleason score 3+4=7b); A: maximum intensity projection (MIP), B+C: PET, D+E: fused PET/CT images.

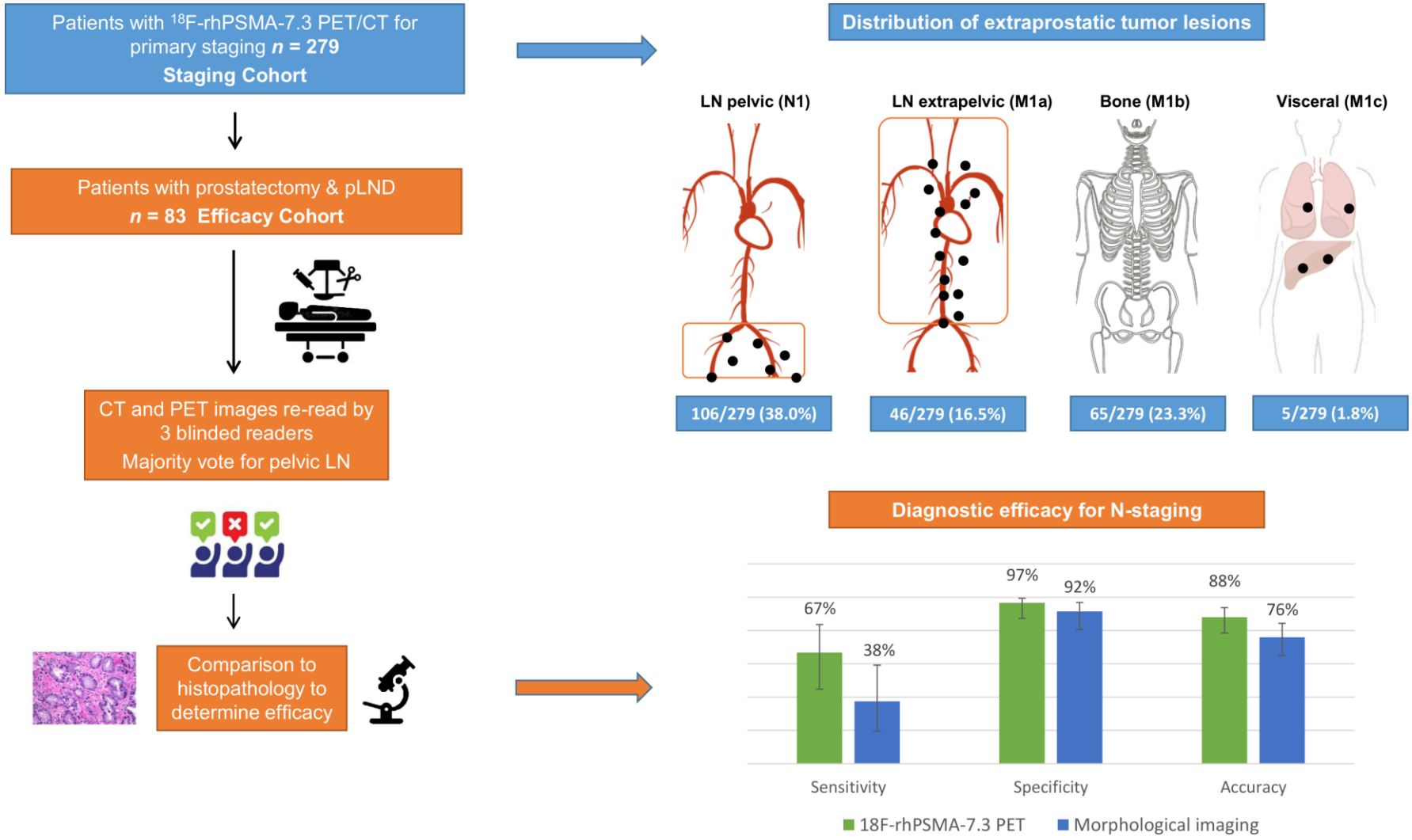

Graphical Abstract

RESULTS

Reader-based Diagnostic Performance

Patient-based Analysis. Data from Reader 1 demonstrated that ^{18}F-rhPSMA-7.3 positron emission tomography (PET) detected 16 out of 24 patients with histologically verified lymph node metastasis while 3 of 59 patients without lymph node metastases were positive on ^{18}F-rhPSMA-7.3. For Reader 2, these were 17/24 and 2/59, respectively and for Reader 3, these were 16/24 and 3/59, respectively. Morphological imaging true positive rates were 7/24 for Reader 1, 10/24 for Reader 2 and 14/24 for Reader 3, while false positives were 3/59, 6/59 and 9/59, respectively. The patient-based sensitivity, specificity, and accuracy of ^{18}F-rhPSMA-7.3 PET and for morphological imaging for each reader are presented in Table 3.

Right vs. Left-side Analysis. When considering the right- vs. left-side analysis, data from Reader 1 demonstrated that ^{18}F-rhPSMA-7.3 PET detected 23 out of 33 patients with histologically verified lymph node metastasis while 3 of 133 patients without lymph node metastases were positive on ^{18}F-rhPSMA-7.3. For both Reader 2 and Reader 3 the rates of true positive were 23/33 and false positive were 4/13. Morphological imaging true positive rates were 7/33 for Reader 1, 10/33 for Reader 2 and 14/33 for Reader 3, while false positives were 3/133, 8/133 and 13/133, respectively. The right- vs. left-based sensitivity, specificity, and accuracy of ^{18}F-rhPSMA-7.3 PET and for morphological imaging for each reader are presented in Table 3.

Template-Based Analysis. When considering the template-based analysis, data from Reader 1 demonstrated that ^{18}F-rhPSMA-7.3 PET detected 30 out of 48 patients with histologically verified lymph node metastasis while 10 of 420 patients without lymph node metastases were positive

on ^{18}F-rhPSMA-7.3. For Reader 2 these were 31/48 and 10/420, respectively and for Reader 3 these were 34/48 and 10/420, respectively. Morphological imaging true positive rates were 5/48 for Reader 1, 9/48 for Reader 2 and 9/48 for Reader 3, while false positives were 4/420, 9/420 and 13/420, respectively. The template-based sensitivity, specificity, and accuracy of ^{18}F-rhPSMA-7.3 PET and for morphological imaging for each reader are presented in Table 3.

Location of lesions	N patients
N0, M0	156
N1, M0	42
N0 or 1, M1a=1, M1b=0, M1c=0	15
N0, M1a=0, M1b=1, M1c=0	15
M1c=1	5
N0 or 1, M1a+M1b=1 M1c=0	26
N1, M1a=0, M1b=1, M1c=0	20

Supplementary Table 1. Patient-based pattern of lesion distribution

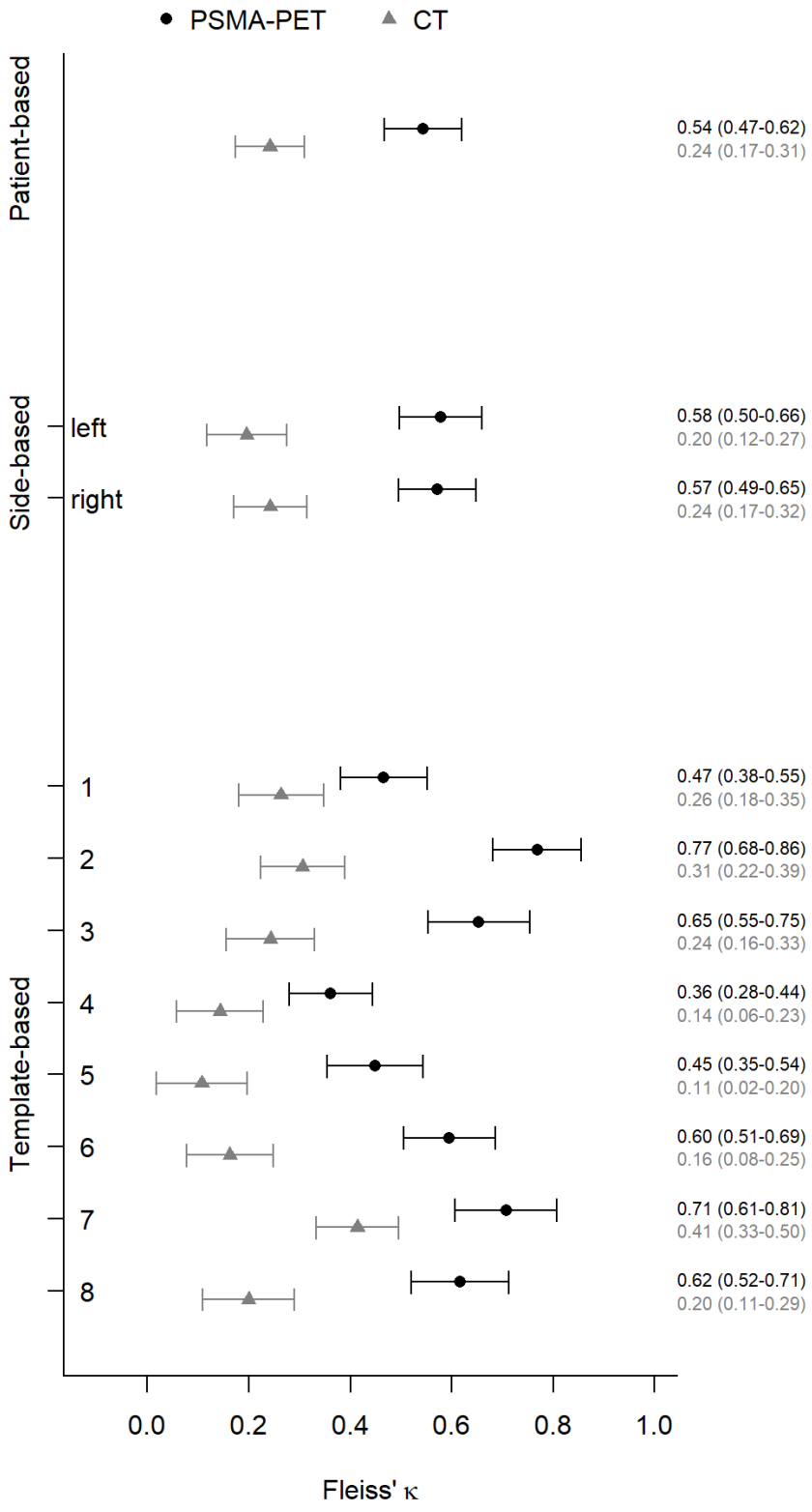

Supplementary Figure 1. Inter-reader agreement for ^{18}F-rhPSMA-7.3 and morphological imaging (CT)

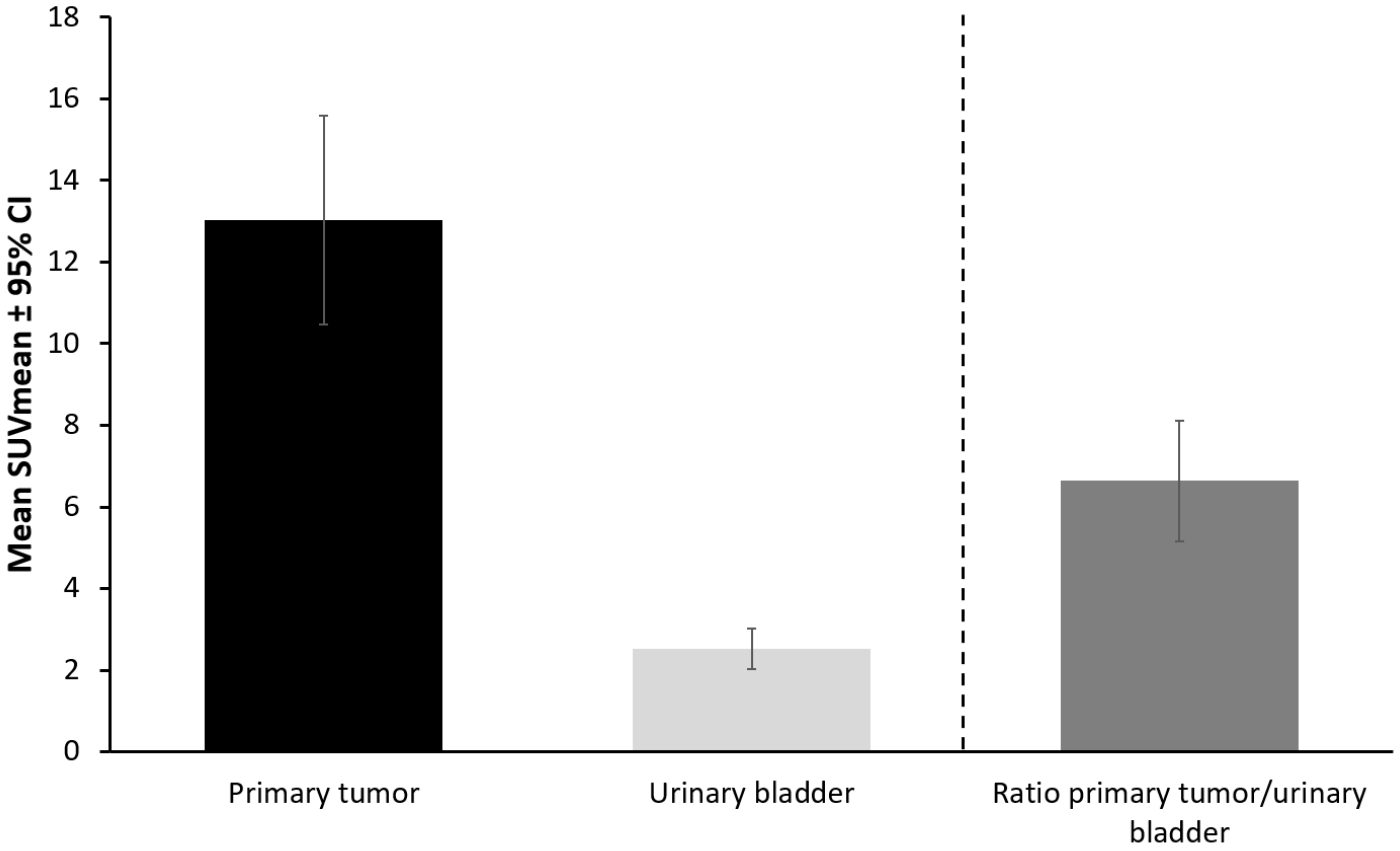

Supplementary Figure 2. ^{18}F-rhPSMA-7.3 uptake in primary tumor compared with bladder retention. Data are shown as mean SUVmean with 95% confidence intervals.